J. metamorphic Geol. 1987, 5, 291-306

Metamorphism in the Olary Block, South Australia: compression with cooling in a Proterozoic fold belt

G.L. CLARKE, M. GUIRAUD, R. POWELL AND J.P. BURG*,
Department of Geology, University of Melbourne, Parkville, Victoria, 3052, Australia

Abstract. The sedimentary and igneous rocks comprising the lower Proterozoic Olary Block, South Australia, were deformed and metamorphosed during the mid-Proterozoic 'Olarian' Orogeny. The area is divided into three zones on the basis of assemblages in metapelitic rocks, higher grade conditions occurring in the south-east. Mineral assemblages developed during peak metamorphism, which accompanied recumbent folding, include andalusite in Zones I and II and sillimanite in Zone III. Upright folding and overprinting of mineral assemblages occurred during further compression, the new mineral assemblages including kyanite in Zone II and kyanite and sillimanite in Zone III. The timing relationships of the aluminosilicate polymorphs, together with the peak metamorphic and overprinting parageneses, imply an anticlockwise *P–T* path for the 'Olarian' Orogeny, pressure *increasing* with cooling from the metamorphic peak.

Key-words: aluminosilicate polymorphs; perturbed geotherm; *P–T* path; Olary Block, Willyama Complex

List of abbreviations used in the text and figures

A = aluminosilicate
And = andalusite
B = biotite
C = cordierite
Chl = chlorite
Ct = chloritoid
Fib = fibrolitic sillimanite
G = garnet
Kf = K-feldspar
Ky = kyanite
Mu = muscovite
Qtz = quartz
S = staurolite
Sill = sillimanite

*Present address: Centre Géologique et Géophysique, Université des Sciences et Techniques du Languedoc, Place Eugène Bataillon, 34060 Montpellier Cedex, France.

INTRODUCTION

The anticlockwise pressure–temperature (*P–T*) paths of the early to middle Proterozoic domains of Australia (e.g. Phillips & Wall, 1981; Warren, 1983; Etheridge, Rutland & Wyborn, 1985) are incompatible with the rapid crustal thickening followed by isostatic uplift that is inferred for modern collisional orogens (England & Richardson, 1977; Thompson & England, 1984). Such a Proterozoic terrain is the Willyama Complex (Mawson, 1912; Vernon, 1969), which comprises metasedimentary and meta-igneous sequences (Willis, Brown, Stroud & Stevens, 1983). It is informally divided into the Olary Block and the Broken Hill Block (Fig. 1), arbitrarily along the New South Wales–South Australia border (Thompson, 1976), or along a geophysical boundary representing the probable south-western extension of the Pliocene Mundi Mundi Fault (Stevens, 1986).

The Broken Hill Block is a low to intermediate pressure terrain with regional metamorphic grade increasing from the north-west, where metapelitic rocks contain andalusite + muscovite, to the south-east where metapelitic rocks contain sillimanite + K-feldspar + garnet + cordierite and metabasic rocks contain orthopyroxene + clinopyroxene (Phillips & Wall, 1981). An anticlockwise *P–T* path, terminating in isobaric cooling has been inferred for the Broken Hill Block (Phillips & Wall, 1981). In contrast, little has been published on the metamorphism in the Olary Block. This paper presents the results of the metamorphic part of a structural/metamorphic study of the Olary

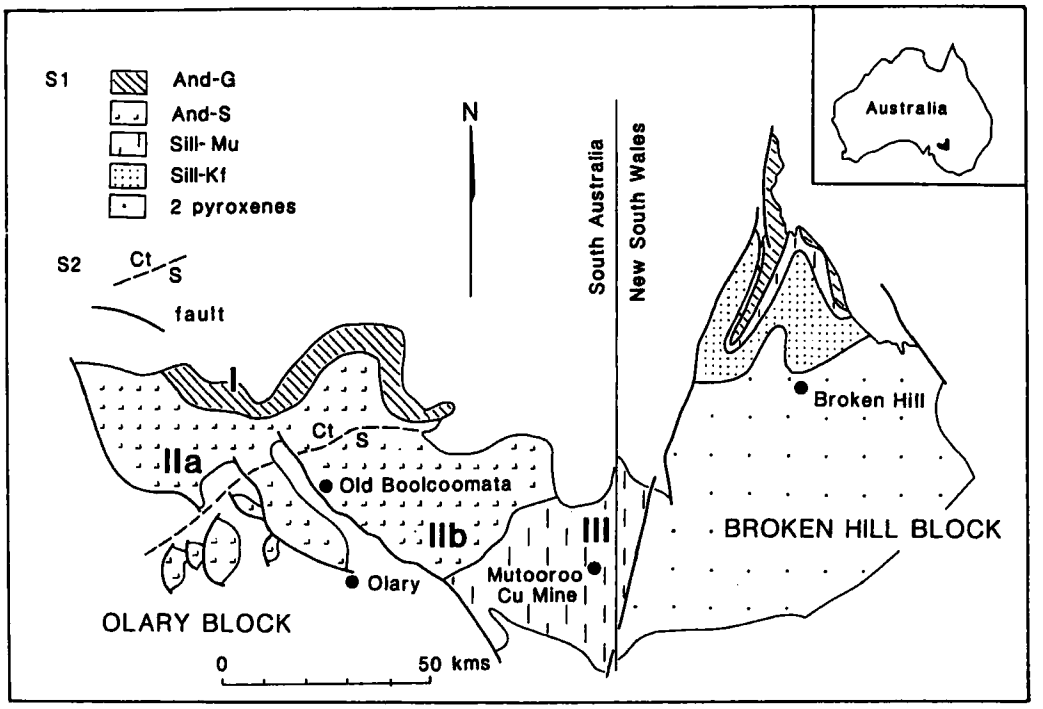

Fig. 1. Sketch map of the Willyama Complex showing the distribution of metamorphic zones. Zonation for the Broken Hill Block is after Phillips (1978). I, IIa, IIb and III refer to the zones defined in the text for the Olary Block.

Block (see also Clarke, Burg & Wilson, 1986). The regional metamorphic relationships within the Olary Block are outlined, the timing relationships of metamorphism with respect to structure are discussed, and the likely *P–T* path of metamorphism is inferred. The tectonothermal consequences of these results are also discussed.

REGIONAL GEOLOGY OF THE OLARY BLOCK

The gneisses and schists of the Olary Block occur as a series of semi-isolated blocks which are in fault contact with the upper Proterozoic 'Adelaidean' sedimentary succession (Mawson & Sprigg, 1950; Sprigg, 1952) to the west and south-west, but are onlapped by 'Adelaidean' rocks to the north and north-east (Forbes & Pitt, 1980). The succession in the Olary Block has been divided into five conformable rock suites, which can be correlated with the lower Proterozoic Willyama Supergroup of the Broken Hill Block (Willis *et al.*, 1983). It does not contain any component of Archaean basement (cf. Glen, Laing, Parker & Rutland, 1977).

Resolution of the stratigraphy in the Olary Block has allowed analysis of the regional structure; the outcrop geometry is explained in terms of a refolded recumbent terrain (Clarke *et al.*, 1986). An L_1 mineral and elongation lineation, indicating a D_1 transport direction, has a consistent trajectory on a regional scale at a high angle to recumbent F_1 fold hinge lines. Inverted limbs which are several kilometres long suggest F_1 folds of a similar scale. S_1 cleavage-bedding relationships combined with stratigraphical younging directions indicate a south-eastward directed shear during F_1 fold development. The S_1 mineral fabric associated with the recumbent folds is folded about upright F_2 folds. S_2 is nearly vertical or is steeply dipping toward the north-west; it is consistent with F_2 folds being produced by continued compression in the same sense and direction as inferred for the recumbent deformation event, D_1. This continued compression giving rise to D_1 and D_2 comprises the 'Olarian' Orogeny. The subparallelism of the trend of F_1 and F_2 axes, and

a consistent shear direction within the Olary Block and Broken Hill Block, suggest that the two areas are part of a single terrain (Clarke *et al.*, 1986).

At least two phases of granitoids intrude the metasediments. Syntectonic plutonism is most prevalent in the southern part of the studied area, and includes albite-rich and lesser microcline-rich granitoids. Liverton (1967) considered the microcline-rich granitoids to be possibly syn-D_1. However, P.M. Ashley (personal communication, 1986) considers them to be synchronous with the albite-rich granitoids, which post-date D_1 but contain an S_2 foliation (Forbes & Pitt, 1980; 1987; Clarke *et al.*, 1986). One of these albite-rich granitoids has been dated at 1579 ± 2 (U/Pb on zircons) by Ludwig & Cooper (1984). Accompanying the syntectonic granitoids are numerous and widely distributed sodic-rich pegmatities. A later phase of granitic to granodioritic intrusions post-dates D_2 (Forbes & Pitt, 1980; 1987).

The area is cut by retrograde shear zones which post-date both the 'Olarian' orogeny and the latest granitoids but which began prior to deposition of the upper Proterozoic 'Adelaidean' sediments (Vernon & Ransom 1971; Etheridge & Cooper, 1981). The Cambrian 'Delamerian' Orogeny caused the folding of the 'Adelaidean' sequence and resulted in the development of discrete zones of high strain within the lower Proterozoic gneisses (Clarke *et al.*, 1986). Movement on these zones resulted in the outcrop pattern in the Olary Block.

METAMORPHIC GEOLOGY

Attention is focused on the metapelitic rocks because they are the most useful in inferring the metamorphic history of the Olary Block. The metapelitic rocks contain two foliations, S_1 and S_2, with S_2 usually dominant. The dominance of S_2 makes the deduction of S_1 mineral assemblages a considerable problem. The minerals associated with S_1 are considered by us to include those minerals that display apparent reaction relationships with minerals forming the S_2 fabric. Other minerals that may form part of the S_1 assemblage are those that form porphyroblasts wrapped around by the S_2 fabric. Such textural relationships rarely provide an unequivocal timing of mineral growth with respect to the development of a tectonic fabric (Bell & Rubenach, 1983; Bell, Rubenach & Fleming, 1986). Nevertheless, these observations, with due consideration of the metamorphic implications of possible mineral parageneses (Vernon, 1978), have been used to infer the S_1 parageneses. The abundant matrix minerals are included in both S_1 and S_2 parageneses.

Three zones can be distinguished using inferred S_1 assemblages (Fig. 1). To the north, Zone I is characterized by coexisting andalusite, garnet and biotite; Zone II by coexisting andalusite, staurolite and biotite; and Zone III, the poorly outcropping sequence surrounding the Mutooroo Copper mine to the south, by coexisting sillimanite, staurolite and biotite. These assemblages also involve quartz and muscovite. This zonation suggests that the rocks exposed in the south were metamorphosed at higher grade than those in the north, although the Zone I assemblage appears to be anomalous, as discussed later. This is consistent with the previous interpretation by Spry (1977) and the south-eastward increase in metamorphic grade in the Broken Hill Block (Binns, 1964; Phillips & Wall, 1981).

In Zones I and II, S_1 andalusite is pseudomorphed by S_2 fibrolitic sillimanite except in the vicinity of the syntectonic granitoids. Localized contact metamorphic zones of less than 5 km radius occur around these granitoids and are superimposed upon the S_1 zonation. In these contact zones prismatic sillimanite, aligned within S_2, replaces S_1 andalusite. Zone II can be subdivided on the basis of S_2 chloritoid (Zone IIa) and S_2 staurolite (Zone IIb). Staurolite is also present with S_2 kyanite in Zone III (see also Thompson, 1976; Spry, 1977; Forbes & Pitt, 1980).

Petrography

Zone I

The metapelitic rocks of Zone I contain centimetre-scale andalusite porphyroblasts, enveloped by a pervasive S_2 mineral fabric defined by muscovite and chlorite, with less garnet and biotite or fibrolitic sillimanite. Biotite occurs as large euhedral flakes that define a relict S_1 fabric oblique to S_2, although, in some rocks biotite forms part of the S_2 mineral fabric, in which case both fibrolitic sillimanite and corroded andalusite are separated from the 'matrix' of the rock by a halo of muscovite oriented within S_2. Muscovite and biotite are commonly kinked by S_2. Biotite is commonly pseudomorphed by muscovite, chlorite and ilmenite. Garnet may contain elongate inclusions that are aligned oblique to the envel-

oping S_2 fabric, but overall is inclusion-poor. Garnet may be locally partially pseudomorphed by poorly oriented chlorite. The andalusite blasts are commonly pseudomorphed by fine-grained white mica and fibrolitic sillimanite, and may contain fine-grained corundum. Fibrolitic sillimanite also forms tails from corroded andalusite grains, drawn out in S_2. The blasts display variable orientations within S_2; in some localities they are well oriented sub-parallel to an F_2-bedding intersection lineation (Fig. 6 in Clarke *et al.*, 1986), but the majority are randomly oriented within the S_2 axial plane. Non-graphitic carbonaceous material is disseminated throughout the matrix, and is accompanied by pyrrhotite with less pyrite; these can be important constituents of some rocks. Andalusite commonly occurs as chiastolite in these carbonaceous rocks.

Zone IIa

Metapelitic rocks in this zone are characterized by chloritoid schists. Any evidence of an earlier schistosity within these rocks has been destroyed by the intensity of development of the S_2 fabric (e.g. Fig. 2a). In garnet-bearing assemblages, a strong S_2 mineral fabric is defined by muscovite, chlorite and chloritoid, enveloping garnet and biotite, which are pseudomorphed by the same minerals as in Zone I. Chlorite and chloritoid may also display poor orientation and S_2 inclusion trails which suggest some static, post S_2 growth. Biotite and chloritoid have ragged grain contacts where the two are adjacent. Rare fibrolitic sillimanite is entirely enclosed in muscovite. Garnet-free assemblages contain corroded, centimetre-scale andalusite porphyroblasts and abundant fibrolitic sillimanite. The andalusite blasts frequently contain fine-grained inclusions of corundum, and are pseudomorphed by poorly oriented muscovite, chloritoid, fibrolitic sillimanite and chlorite. Enveloping these corroded blasts is an anastomosing S_2 involving muscovite, fibrolitic sillimanite, chlorite and chloritoid. Biotite flakes are enveloped by S_2, and, as in Zone I, they are pseudomorphed by the muscovite and chlorite that define S_2.

Zone IIb

Most metapelitic rocks contain centimetre-scale andalusite porphyroblasts which are enveloped by S_2, as in Zone IIa. This foliation is defined by muscovite, chlorite and biotite, and contains garnet and rarely, corroded staurolite. The S_2 foliation abuts garnet grains, some of which contain elongate inclusions. In some grains these inclusions are parallel to S_2, but in other grains are aligned oblique to S_2. These relationships are consistent with syn- to post-S_2 garnet growth. Flakes of remnant biotite aligned within S_2 are usually pseudomorphed by chlorite and muscovite, as in Zone I, whereas biotite flakes within andalusite blasts are aligned oblique to S_2 and preserve an S_1 fabric. The stratigraphical horizon containing the carbonaceous schists outcrops as graphitic schist.

Other metapelitic rocks differ from the above in containing aluminosilicate aggregates that are separated from the matrix assemblage by a halo of muscovite. In the matrix of these rocks biotite does not appear to be retrogressed, and is inferred to have been stable in S_2. The muscovite halo is oriented in S_2 (Fig. 2f) and contains numerous small inclusions of corundum. The aluminosilicate aggregates are petrographically complex. The aggregates have cores of andalusite + staurolite, and have rims of chloritoid + fibrolitic sillimanite. Staurolite in the cores may define a weak S_1 foliation oblique to S_2, but is typically unoriented. The chloritoid + fibrolitic sillimanite haloes form part of the S_2 fabric. In thin section, the aggregates are seen to also contain biotite replaced by chlorite and muscovite. Chloritoid has ambiguous timing relationships with the abundant staurolite, the small grains of corundum, the pseudomorphous fibrolitic sillimanite and fine-grained white mica after andalusite.

Close to the syntectonic granitoids the aggregates may contain *all three* aluminosilicate polymorphs (Fig. 2b & c). In these rocks, andalusite is pseudomorphed by prismatic sillimanite and lesser kyanite, and the chloritoid + fibrolitic sillimanite haloes are less well developed. Immediately adjacent to the granitoids, the aggregates are composed of prismatic sillimanite + kyanite + staurolite. The peripheries of these aggregates contain staurolite and sillimanite oriented within S_2; kyanite has a random orientation in the cores and so is probably not related to a tectonic fabric. However, Whittle (1949) described kyanite + muscovite schists within this zone (Old Boolcoomata area, Fig. 1), with kyanite as part of the foliation called S_2 here.

Zone III

Within this poorly outcropping zone, staurolite schists containing either kyanite and sillimanite

or garnet occur (Fig. 2d & e). In these rocks, S_2 is a crenulation cleavage, which tightly refolds an earlier fabric involving staurolite + biotite + muscovite + quartz; it envelops garnet where present. Kyanite and prismatic sillimanite appear to have been stable with staurolite, all three defining S_2. Sillimanite defines a rodding fabric within the S_2 axial plane, whereas kyanite lies within S_2, but does not define a lineation. Kyanite contains inclusion trails that involve elongate quartz grains, presumably defining a relict S_1. Biotite is commonly pseudomorphed by chlorite which, in some instances, is poorly oriented.

Mineral chemistry

Analyses were performed on the Melbourne University Jeol JXA-5A electron microprobe operating with an accelerating voltage of 15 kV and a beam width of 10–15 μm. The data were reduced according to Ferguson & Sewell (1980). We present below the major features of the chemistry of the minerals in the metapelitic rocks. Representative analyses are given in Table 1.

Muscovite

Muscovite contains minor amounts of paragonite and phengite, and is commonly alkali deficient. The composition is approximately the same in all zones.

Biotite

In biotite, $X_{Fe} = Fe^{2+}/(Fe^{2+}+Mg)$ ranges from 0.50 to 0.69 within the Olary Block, but is rather constant in each rock. The highest X_{Fe} values are mainly restricted to Zone I, whereas the lowest X_{Fe} values are found in Zone III. Zone IIa and IIb display intermediate values, generally with $X_{Fe} < 0.63$ in Zone IIb and $X_{Fe} > 0.63$ in Zone IIa. The MnO content of biotite is very small, but seems related to the X_{Fe} variations; it ranges from 0.14 to 0.22 wt % in Zone I, whereas it is just above the detection limit in Zone III. Alkali deficiency is a general feature of the retrogressed biotites.

Chlorite

Chlorite is ripidolite with values of Si (for 28 O) ranging from 5.03 to 5.26 for all the zones. Chlorite formed by retrogression of biotite has greater values of Si and K; interlayering of chlorite with muscovite may affect the analysis. Chlorite commonly records the same X_{Fe} value as the biotite. Moreover, the variations of X_{Fe} and MnO in chlorite between the different zones are the same as the variations shown by biotite. This chemical similarity of the chlorite and biotite may be due to incomplete equilibration of Fe, Mg and Mn between chlorite and the other S_2 minerals during the development of the S_2 mineral assemblages.

Garnet

In all the zones, the garnet is almandine-rich and is slightly zoned; from core to rim, spessartine content generally decreases as almandine and pyrope contents increase, with grossular content remaining constant. The same geographical variation of MnO in biotite and chlorite is shown by garnet. In Zones I and IIa, the spessartine content ranges between 0.14 and 0.23, whereas in Zones IIb and III, it ranges from 0.04 to 0.14. In addition to the MnO variation, pyrope and almandine contents increase, X_{Fe} decreases and grossular content remains constant from Zone I and IIa to Zone IIb and III.

Chloritoid

In chloritoid, the X_{Fe} values in Zone IIa range from 0.85 to 0.90, but are constant in each analysed rock; the highest X_{Fe} values are found in the samples showing the highest X_{Fe} values for garnet, biotite and chlorite. With MnO values ranging from 0.21 to 0.60 wt %, chloritoid is the most manganiferous mineral after garnet.

Staurolite

In staurolite, the X_{Fe} values have a range similar to chloritoid, from 0.84 to 0.89, but as for chloritoid, the X_{Fe} values are constant in each rock sample. Charge balance for staurolite does not lead to Fe^{3+} in structural formulae. ZnO values are between 0.40 and 0.93 wt %.

Aluminosilicate

In aluminosilicate, Mn_2O_3 is negligible in all the zones. Values up to 0.9% Fe_2O_3 occur, with no significant difference between the polymorphs.

Inferred mineral parageneses

Most metapelite assemblages of the Olary Block may be considered, in the first instance, in terms of the model system K_2O–FeO–

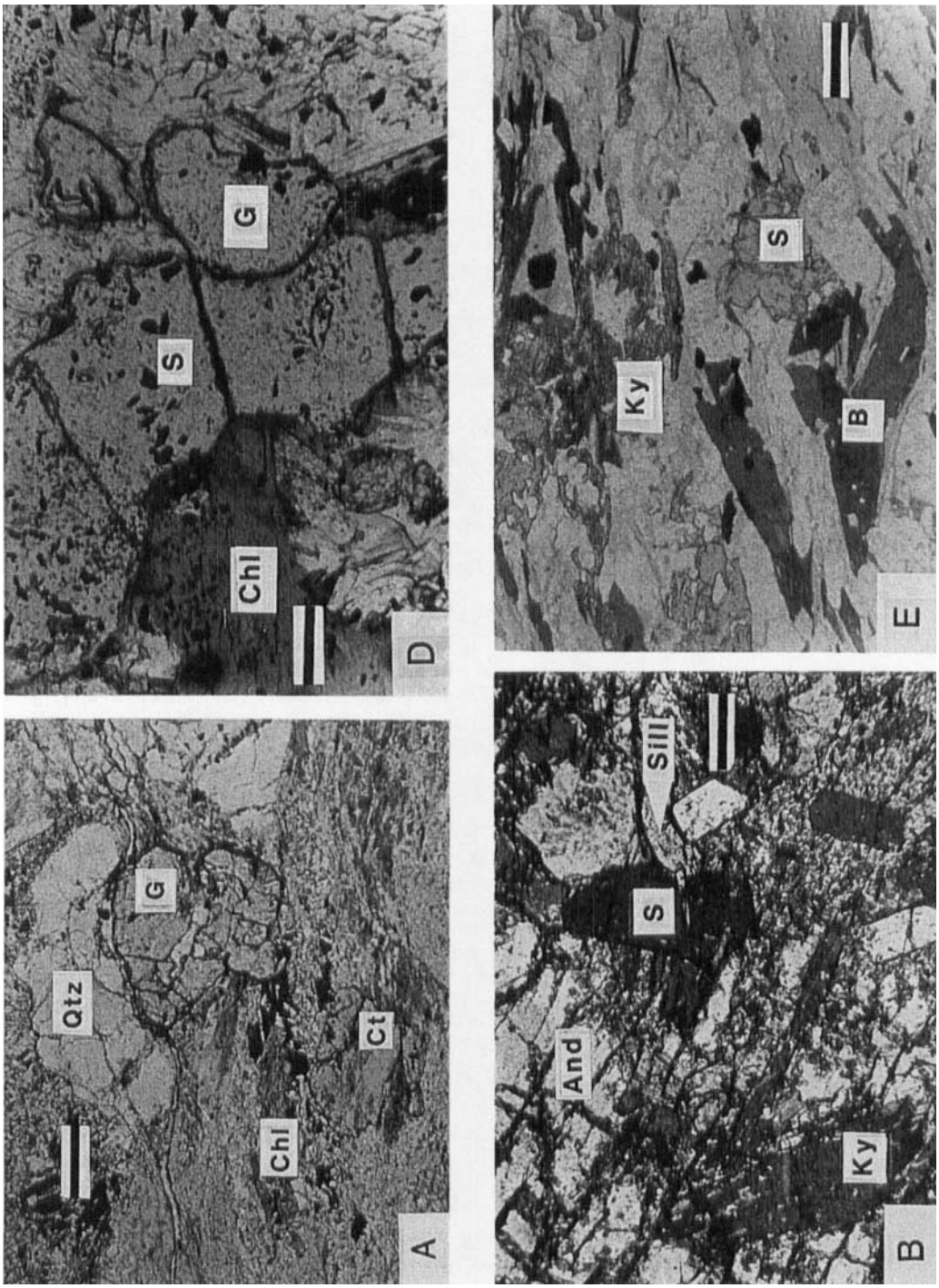
A
Qtz
G
Chl
Ct
B
And
Sill
S
Ky
D
G
S
Chl
E
Ky
S
B

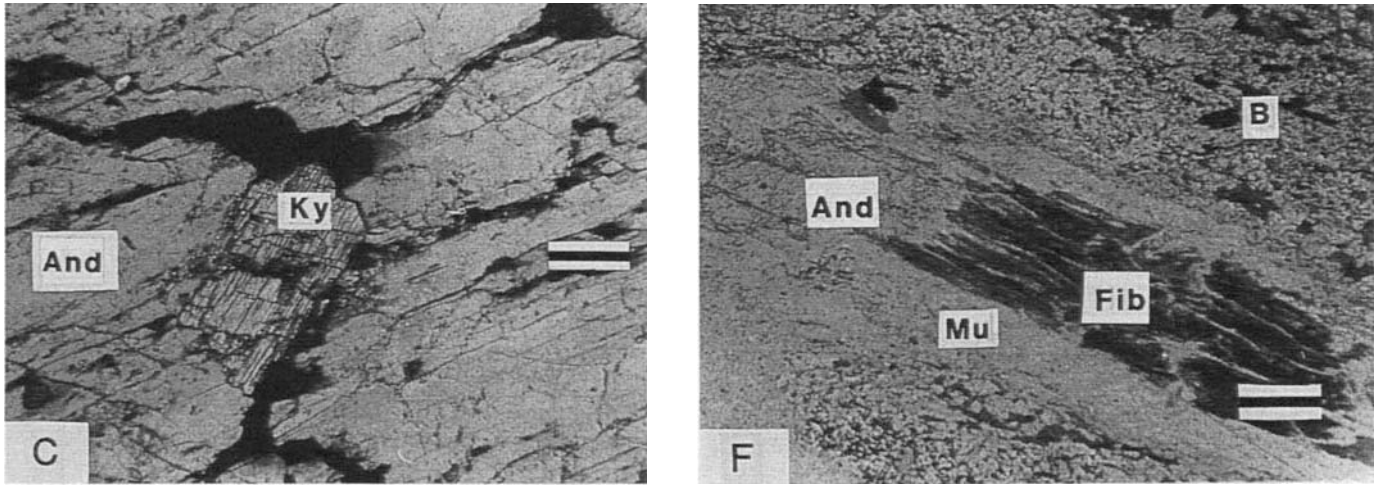

Fig. 2. Plane-polarized light photomicrographs of thin sections from Olary Block. **a** Zone IIa garnet + chlorite + chloritoid assemblage. Chloritoid and chlorite form part of the S_2 foliation which is oriented east–west in the photomicrograph. Scale bar = 0.5 mm. **b** Zone IIb aluminosilicate aggregate close to syntectonic granitoid. S_2 kyanite, sillimanite and staurolite in metastable S_1 andalusite. Andalusite forms most of the photomicrograph. Scale bar = 0.5 mm. **c** Zone IIb kyanite–andalusite relationships within aluminosilicate aggregate close to granitoid. Scale bar = 0.5 mm. **d** Zone III S_2 staurolite + chlorite + garnet assemblage. Scale bar = 0.15 mm. **e** Zone III metastable kyanite + biotite + staurolite assemblage; biotite is retrogressed to chlorite elsewhere in the sample. Scale bar = 0.5 mm. **f** Zone IIb S_1 andalusite and S_2 fibrolitic sillimanite separated from matrix pelite biotite by a halo of muscovite. Scale bar = 0.5 mm.

Table 1. Representative analyses of the minerals from the Olary Block. I, IIa, IIb and III refer to the zones defined in the text. Fe^{3+} in garnet is estimated on the basis of 16 cations and 24 oxygens. Structural formulae of staurolite are calculated on 46 oxygens. Other structural formulae are calculated on the basis of all iron as FeO, and on 22 O for muscovite and biotite, 28 O for chlorite and 12 O for chloritoid. $X_{Fe} = Fe^{2+}/(Fe^{2+}+Mg)$

	G I core	G I rim	G IIa core	G IIa rim	G IIb core	G IIb rim	G IIb core	G IIb rim	G III core	G III rim
SiO_2	36.35	36.65	37.54	37.42	37.13	37.53	36.18	36.33	37.40	37.45
TiO_2	0.14	0.05	0.04	0.00	0.00	0.30	0.01	0.01	0.03	0.04
Al_2O_3	20.55	20.80	20.62	20.73	21.17	20.98	20.93	20.81	21.04	20.90
Cr_2O_3	0.01	0.05	0.00	0.12	0.08	0.00	0.07	0.05	0.03	0.02
FeO	32.06	34.36	31.86	33.97	34.70	36.00	33.26	33.60	32.23	33.87
MnO	7.86	7.13	10.25	7.30	5.98	2.78	6.07	5.49	2.89	2.80
MgO	0.76	1.32	0.91	1.33	1.85	2.10	1.79	1.72	2.46	2.74
CaO	1.51	1.10	0.54	0.64	0.97	2.06	1.24	0.99	3.21	2.97
Sum	99.24	101.46	101.76	101.51	101.88	101.74	99.55	99.01	100.29	100.79
Si	5.997	5.913	6.053	6.032	5.940	5.989	5.916	5.976	6.008	5.987
Al^{iv}	0.003	0.087	0.000	0.000	0.060	0.011	0.084	0.024	0.000	0.013
Tet	6.000	6.000	6.053	6.032	6.000	6.000	6.000	6.000	6.008	6.000
Al^{vi}	3.992	3.867	3.917	3.937	3.930	3.934	3.948	4.009	3.982	3.924
Ti	0.017	0.006	0.005	0.000	0.000	0.036	0.001	0.001	0.004	0.005
Cr	0.001	0.006	0.000	0.015	0.010	0.000	0.009	0.007	0.004	0.003
Fe^{3+}	0.000	0.201	0.000	0.000	0.120	0.006	0.125	0.006	0.000	0.078
Fe^{2+}	4.427	4.437	4.296	4.580	4.522	4.797	4.423	4.616	4.464	4.451
Mn	1.098	0.974	1.400	0.997	0.810	0.376	0.841	0.765	0.393	0.379
Mg	0.187	0.317	0.219	0.320	0.441	0.500	0.436	0.422	0.589	0.653
Ca	0.267	0.190	0.093	0.111	0.166	0.352	0.217	0.174	0.552	0.509
Sum	15.987	16.000	15.983	15.992	16.000	16.000	16.000	16.000	15.996	16.000
alm	0.740	0.750	0.715	0.762	0.761	0.796	0.748	0.772	0.744	0.743
spe	0.184	0.165	0.233	0.166	0.136	0.062	0.142	0.128	0.066	0.063
pyr	0.031	0.054	0.036	0.053	0.074	0.083	0.074	0.071	0.098	0.109
gro	0.045	0.032	0.015	0.018	0.028	0.058	0.037	0.029	0.087	0.085
X_{Fe}	0.959	0.933	0.952	0.935	0.911	0.906	0.910	0.916	0.883	0.872

$MgO–Al_2O_3–SiO_2–H_2O$ (KFMASH). Since quartz and muscovite are in excess in the rocks discussed here, and H_2O is considered to have been in excess, the assemblages can be shown in the AFM projection (Thompson, 1957). This projection is inappropriate for the aluminosilicate aggregates, which contain corundum and not quartz. A factor that restricts the value of the AFM projection is the importance of Mn, occurring in garnet and to a smaller extent in chloritoid, in many of the Olary Block metapelites. It is still useful, however, to represent the mineral parageneses in the AFM projection, because it allows a discussion of the metamorphism of the Olary Block in the light of a considerable body of previous work. A summary of the inferred parageneses for the Olary Block, in AFM projection, is shown in Fig. 3.

Within all three Zones of the Olary Block, an S_1 biotite–aluminosilicate tie-line is cut by tie-lines involving S_2 chlorite and at least one of the Fe-rich minerals, garnet, chloritoid or staurolite. Biotite and aluminosilicate persist together in S_2 only metastably; the unstable juxtaposition of the two phases in S_2 is well illustrated in Fig. 2f where both andalusite and fibrolitic sillimanite are separated from biotite by muscovite. S_2 chlorite, stable with some of biotite, garnet, chloritoid, staurolite and aluminosilicate, allows the zonal S_2 assemblages to be represented in AFM by three-phase fields principally differentiated by bulk Al/(Fe+Mg) composition. Depending on bulk rock composition, biotite and/or aluminosilicate are metastable and so are retrogressed during the development of S_2.

Table 1. *(continued)*

	Mu I	Mu IIa	Mu IIb	Mu III	B I	B IIa	B IIa	B IIa	B IIb	B IIb	B III	Chl I
SiO_2	47.58	47.08	45.83	47.19	33.32	34.31	33.50	36.07	34.33	34.44	34.49	23.48
TiO_2	0.42	0.45	0.57	0.41	2.04	2.58	1.11	1.01	1.29	1.41	2.00	0.10
Al_2O_3	35.31	36.48	34.36	34.23	19.23	18.98	18.33	20.60	18.65	18.31	17.47	21.92
Cr_2O_3	0.07	0.05	0.03	0.06	0.00	0.09	0.00	0.01	0.00	0.00	0.05	0.00
FeO	1.65	1.45	2.64	2.35	23.74	22.20	23.53	23.36	21.37	20.64	18.94	30.24
MnO	0.06	0.04	0.00	0.01	0.14	0.04	0.08	0.13	0.06	0.09	0.03	0.25
MgO	0.65	0.37	0.43	0.67	6.99	7.17	6.66	6.02	9.86	9.81	10.23	8.86
CaO	0.00	0.00	0.00	0.00	0.00	0.02	0.00	0.00	0.00	0.00	0.16	0.18
ZnO	0.00	—	0.11	—	0.00	—	—	0.35	—	—	—	—
Na_2O	0.74	1.13	1.26	1.10	0.14	0.21	0.22	0.36	0.28	0.36	0.28	0.11
K_2O	9.17	9.23	9.24	9.58	8.08	7.43	8.22	6.94	8.42	8.59	8.04	0.14
Sum	95.65	92.28	94.47	95.60	93.68	93.03	91.65	94.85	94.26	93.65	91.69	85.28
Si	6.259	6.160	6.173	6.265	5.259	5.376	5.411	5.521	5.325	5.368	5.435	5.262
Al^{iv}	1.741	1.840	1.827	1.735	2.741	2.624	2.589	2.479	2.675	2.632	2.565	2.738
Tet	8.000	8.000	8.000	8.000	8.000	8.000	8.000	8.000	8.000	8.000	8.000	8.000
Al^{vi}	3.732	3.784	3.626	3.619	0.835	0.880	0.900	1.236	0.734	0.730	0.679	3.050
Ti	0.042	0.044	0.058	0.041	0.242	0.304	0.135	0.116	0.150	0.165	0.237	0.017
Cr	0.007	0.005	0.003	0.006	0.000	0.011	0.000	0.001	0.000	0.000	0.006	0.000
Fe^{2+}	0.182	0.159	0.297	0.261	3.134	2.909	3.179	2.990	2.772	2.690	2.496	5.667
Mn	0.007	0.004	0.000	0.001	0.019	0.005	0.011	0.017	0.008	0.012	0.004	0.047
Mg	0.127	0.072	0.086	0.133	1.645	1.675	1.604	1.374	2.280	2.279	2.403	2.960
Ca	0.000	0.000	0.000	0.000	0.000	0.003	0.000	0.000	0.000	0.000	0.027	0.043
Zn	0.000	—	0.011	—	0.000	—	—	0.040	—	—	—	—
Na	0.189	0.287	0.329	0.283	0.043	0.064	0.069	0.107	0.084	0.109	0.086	0.048
K	1.539	1.541	1.588	1.623	1.627	1.485	1.694	1.355	1.666	1.708	1.616	0.040
Sum	13.824	13.895	13.999	13.967	15.545	15.337	15.591	15.236	15.695	15.694	15.554	19.872
X_{Fe}	0.587	0.687	0.775	0.663	0.656	0.635	0.665	0.685	0.549	0.541	0.509	0.657

In Zone I, S_1 to S_2 involves the appearance of the garnet–chlorite tie-line, resulting in garnet and chlorite coexisting with biotite or aluminosilicate. The elongate inclusions oblique to an enveloping S_2 foliation suggests that garnet could be part of the S_1 assemblage in Zone IIa, biotite and andalusite occur as S_1 minerals. Where garnet occurs in S_2, it is enveloped by the S_2 fabric, suggesting the S_1 assemblage garnet + biotite + andalusite, as for Zone I. Another possibility is that the S_1 assemblage for Zone IIa was the same as for Zone IIb. The change from S_1 to S_2 involved the appearance of an S_2 chloritoid–chlorite tie-line, in addition to an S_2 garnet–chlorite tie-line. The S_2 assemblage chloritoid + garnet + chlorite, implies that both S_1 biotite and aluminosilicate were metastable.

In Zone IIb and III, staurolite persists as part of the S_2 fabric and is interpreted as part of the S_1 assemblages aluminosilicate + biotite + staurolite and garnet + biotite + staurolite. The inferred S_2 assemblages for these zones are garnet + chlorite + biotite, garnet + staurolite + chlorite and aluminosilicate + staurolite + chlorite. Thus, S_1 to S_2 involved cutting the S_1 biotite–aluminosilicate tie-line by an S_2 staurolite–chlorite tie-line, and cutting the S_1 staurolite–biotite tie-line by an S_2 garnet–chlorite tie-line.

Aluminosilicate polymorph relationships

The *P–T* path of the Olary Block may be outlined by a consideration of the relative timing of the aluminosilicate polymorphs. Andalusite occurs within S_1 throughout Zones I and II of the Olary Block. The presence of poorly oriented andalusite porphyroblasts suggests that prograde growth continued post-D_1. Overprinting by S_2 fibrolitic sillimanite limits andalusite growth to pre/early S_2. Prismatic sillimanite is stable within S_1 (and S_2) throughout Zone III. The *P–T* locus represented by S_1

Table 1. (*continued*)

	Chl I	Chl IIa	Chl IIa	Chl IIb	Chl IIb	Chl IIb	Chl III	Chl III	Ct IIa	Ct IIa	S IIb	S IIb
SiO_2	24.01	23.20	31.02	23.73	24.53	24.34	23.78	24.50	23.57	24.95	30.22	27.69
TiO_2	0.21	0.34	0.03	0.13	0.05	0.12	0.16	0.05	0.04	0.00	0.19	0.38
Al_2O_3	22.27	23.07	26.98	22.35	22.57	22.56	22.48	22.49	39.80	39.74	50.21	52.49
Cr_2O_3	0.00	0.06	0.05	0.09	0.06	0.08	0.00	0.02	0.07	0.01	0.02	0.00
FeO	30.91	31.01	20.36	29.61	26.75	25.61	25.31	24.74	24.85	24.38	12.59	13.67
MnO	0.28	0.10	0.16	0.11	0.08	0.03	0.06	0.04	0.58	0.21	0.24	0.34
MgO	9.78	10.18	6.14	10.37	13.92	13.09	14.16	14.63	1.50	2.12	0.95	1.38
CaO	0.01	0.02	0.03	0.01	0.01	0.00	0.02	0.00	0.01	0.01	0.03	0.02
ZnO	—	—	—	0.19	—	—	—	—	0.07	0.25	0.93	0.75
Na_2O	0.50	0.03	0.26	0.06	0.08	0.09	0.04	0.04	0.00	0.12	0.14	0.05
K_2O	0.00	0.02	1.99	0.00	0.11	0.07	0.00	0.00	0.00	0.57	0.10	0.02
Sum	87.97	88.03	87.02	86.65	88.16	85.99	86.01	86.51	90.49	92.36	95.62	96.79
Si	5.217	5.035	6.308	5.200	5.186	5.246	5.125	5.220	2.003	2.071	8.552	7.808
Al^{iv}	2.783	2.965	1.692	2.800	2.814	2.754	2.875	2.780	0.000	0.000	0.000	0.192
Tet	8.000	8.000	8.000	8.000	8.000	8.000	8.000	8.000	2.003	2.071	8.552	8.000
Al^{vi}	2.919	2.934	4.772	2.970	2.808	2.975	2.833	2.866	3.985	3.887	16.741	17.247
Ti	0.034	0.055	0.005	0.021	0.008	0.019	0.026	0.008	0.003	0.000	0.040	0.081
Cr	0.000	0.010	0.008	0.016	0.010	0.014	0.000	0.003	0.005	0.001	0.004	0.000
Fe^{2+}	5.617	5.629	3.462	5.426	4.730	4.616	4.562	4.408	1.766	1.693	2.980	3.224
Mn	0.052	0.018	0.028	0.020	0.014	0.005	0.011	0.007	0.042	0.015	0.058	0.081
Mg	3.168	3.294	1.861	3.387	4.387	4.206	4.549	4.647	0.190	0.262	0.401	0.580
Ca	0.002	0.005	0.007	0.002	0.002	0.000	0.005	0.000	0.001	0.001	0.009	0.006
Zn	—	—	—	0.031	—	—	—	—	0.004	0.015	0.194	0.156
Na	0.211	0.013	0.103	0.025	0.033	0.038	0.017	0.017	0.000	0.019	0.077	0.027
K	0.000	0.006	0.516	0.000	0.030	0.019	0.000	0.000	0.000	0.060	0.036	0.007
Sum	20.003	19.964	18.761	19.899	20.021	19.892	20.003	19.956	7.999	8.025	29.092	29.409
X_{Fe}	0.639	0.631	0.650	0.616	0.519	0.523	0.501	0.487	0.903	0.866	0.881	0.848

assemblages passes from the andalusite to the sillimanite field within muscovite + quartz stability, but is otherwise poorly constrained. Superimposed on this locus in Zones I and II is the effect of the post-S_1 to syn-S_2 granitoids, involving the overprinting of andalusite by prismatic sillimanite and, in Zone II, also kyanite.

Delineation of the *P–T* locus represented by the S_2 assemblages requires consideration of the almost ubiquitous fibrolitic sillimanite. However, the presence of kyanite in Zone IIb adjacent to the syntectonic granitoids and its presence in Zone III, with poor orientation and inclusion trails consistent with growth during the flattening D_2 strain (Clarke *et al.*, 1986), suggest that most of the fibrolitic sillimanite grew metastably. We conclude that the S_2 *P–T* locus for the Olary Block lies mostly within the kyanite field, irrespective of the presence of S_2 fibrolitic sillimanite in many rocks. The presence of S_2 kyanite following S_1 sillimanite in Zone III, and S_2 kyanite and sillimanite pseudomorphing S_1 andalusite in Zone IIb, suggests that the Olary Block S_2 assemblages formed from the S_1 mineral assemblages following cooling accompanied by burial.

Petrogenetic grid of the mineral assemblages

Harte & Hudson (1979) have derived a Schreinemakers net for the model pelite system, KFMASH, and located the net in *P–T* space to form a petrogenetic grid (Fig. 4). The purpose of this section is to account for the mineral assemblages in the metapelitic rocks in terms of this grid, for the *P–T* path derived in the last section. This task is made markedly more complicated by the relatively Mn-rich nature of many of the rocks. Mn is partitioned into garnet and, to a smaller extent, chloritoid, enhancing the stability of these minerals (e.g. Osberg, 1971; Hudson & Harte, 1985). In these rocks, the proportion of spessartine in the garnets ranges up to 20%.

The effect on Fig. 4 of the enhancement of the stability of garnet (and chloritoid) by Mn

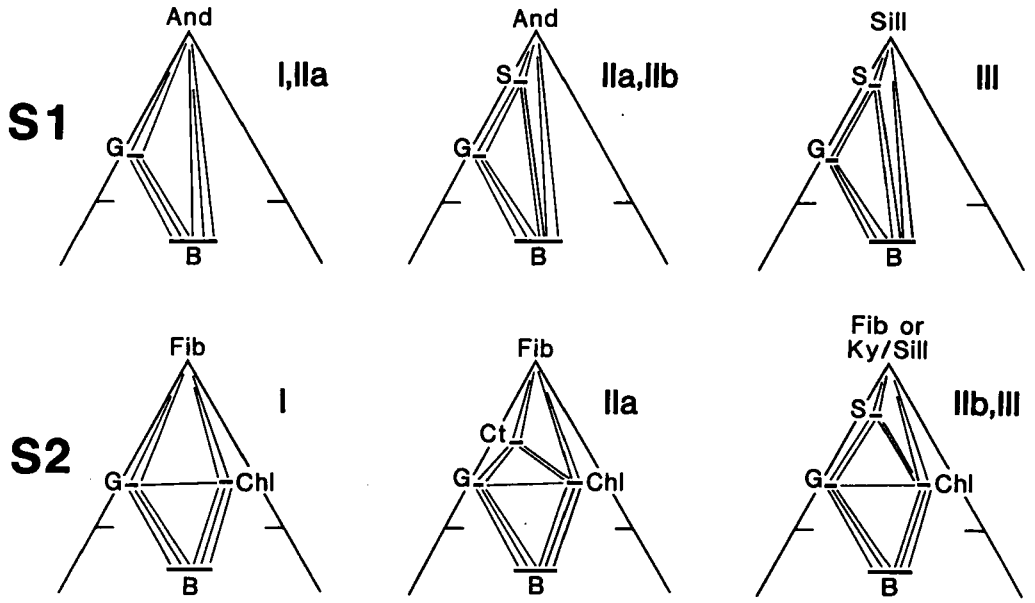

Fig. 3. AFM diagrams (Thompson, 1957) for the interpreted mineral parageneses. Muscovite and quartz are in excess; water is inferred to be in excess. I, IIa, IIb and III refer to the zones defined in the text.

is to expand the stability fields of garnet-bearing (and chloritoid-bearing) assemblages. With the progressive addition of Mn, this is achieved by KFMASH and KFASH intersections on the grid sliding along reactions univariant in KFMnMASH space; KFMASH reactions involving garnet change position in *P–T* space most; KFMASH reactions involving chloritoid and not garnet change less. The directions of movement of the KFMASH and KFASH intersections under the influence of Mn are indicated by arrows in Fig. 4. The positions of the [chloritoid, garnet] intersection and the reactions that radiate from it remain unaffected by the addition of Mn. As a consequence, this intersection is an important reference point in the discussion below; it occurs at approximately 4.5 kbar and 600°C (Hudson & Harte, 1985).

The S_1 assemblages formed in the vicinity of the shaded area that straddles the andalusite = sillimanite boundary in Fig. 4. With aluminosilicate + biotite stable in all zones, the S_1 assemblages formed at temperatures above the reaction staurolite + cordierite = andalusite + biotite, Zones I and II being in the andalusite field, and Zone III in the sillimanite field. With an increase in metamorphic grade to the south, the instability of staurolite with respect to andalusite + garnet + biotite in Zone I and possibly in Zone IIa indicates that Mn displaced the reaction staurolite = aluminosilicate + biotite + garnet to sufficiently low temperatures and pressures that the reaction occurred in the andalusite field, at a lower temperature than the temperature of formation of the rocks. For Zones IIb and III, Mn did not displace this reaction sufficiently to prevent the occurrence of staurolite in these rocks.

With garnet + chlorite stable in all zones, the S_2 assemblages formed above the hatched lines in Fig. 4, noting that these lines are displaced to lower temperatures and pressures as Mn is added to the system. In Zones IIb and III the S_2 assemblage staurolite + garnet + chlorite indicates conditions of formation at higher pressure than [aluminosilicate, cordierite], but at higher temperature than chloritoid = staurolite + garnet + chlorite. For Zone III, the S_2 assemblages must have formed near the kyanite = sillimanite reaction, in order to explain the presence of kyanite and prismatic sillimanite in these assemblages. In contrast to Zones IIb and III, S_2 assemblages from Zone IIa formed at lower temperature than chloritoid = staurolite + garnet + chlorite. If chloritoid + fibrolitic sillimanite is metastable with

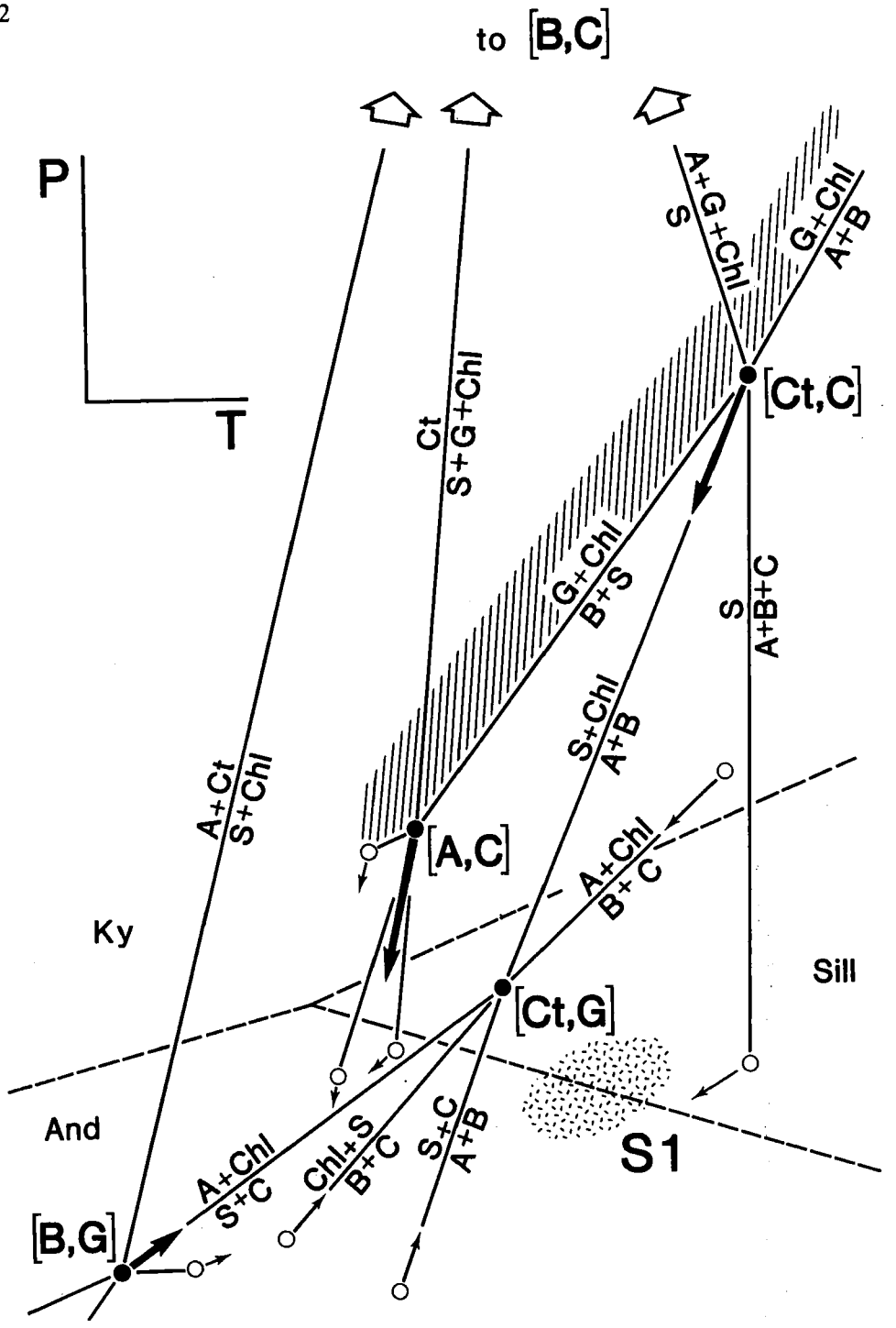

Fig. 4. Qualitative *P–T* diagram after Harte & Hudson (1979) to show the effect of Mn on part of the KFMASH system. (●) KFMASH intersections, with absent phases in brackets. (○) KFASH intersections. The directions of movement of the intersections due to Mn are indicated by large arrows for KFMASH intersections and by small arrows for KFASH intersections. [Chloritoid, garnet] is located according to Hudson & Harte (1985); the aluminosilicate triple point is located according to Holland & Powell (1985). Shaded area indicates the *P–T* conditions of formation of S_1 assemblages. Hatched lines indicate the lower *P*, upper *T* limit of formation of S_2 assemblages.

respect to chloritoid + kyanite, the S_2 assemblages from Zone IIa formed at an even lower temperature, below kyanite + chloritoid = staurolite + chlorite. Zone I S_2 assemblages, like the S_1 assemblages, require a considerable displacement of phase relationships due to Mn, for consistency with assemblages from Zones II and III. If we assume that garnet + chlorite + fibrolitic sillimanite is metastable with respect to garnet + chlorite + kyanite, the development of S_2 occurred at a pressure *higher* than [chloritoid, cordierite].

The *P–T* path for the Olary Block

Given the complexity of the rocks, it is impossible to derive an entirely convincing synthesis of the metamorphic history of the Olary Block; however, it is hard to avoid S_2 metamorphic conditions being at higher pressure than S_1 conditions from the aluminosilicate relationships. There is circumstantial support for this from the model pelite phase relationships. The following synthesis, though speculative, is at least consistent with the data.

It is reasonable to assume that the metamorphic conditions associated with S_1 and S_2 mineral assemblages define geotherms, at least in a general way (Fig. 5). The diachroneity of metamorphic peak conditions of England & Richardson (1977) would not be expected for such a profoundly thermally perturbed situation. Note that the section of the geotherm defined by the S_1 mineral assemblages is constrained only to cross the andalusite = sillimanite reaction, probably at higher pressures given the absence of cordierite in prograde and retrograde assemblages. The section of the S_2 geotherm must just enter the sillimanite field at the high temperature end, but otherwise is poorly constrained, apart from probably lying everywhere in the kyanite field. The proximity and continuity of the zones suggests that the *P–T* paths for the zones should be broadly parallel. This means that although it is conceivable that the change from S_1 to S_2 in Zone III is isobaric, this is not possible for the other zones, particularly Zone IIb. The sort of anticlockwise *P–T* path indicated on Fig. 5, involving limited cooling but an increase in pressure, seems inescapable.

DISCUSSION

The 'Olarian' Orogeny involved a regional south-eastward directed shear strain, with recumbent folding accompanying or slightly preceding peak metamorphic conditions. Continued compression accompanied the development of mineral assemblages to record a slightly increased crustal thickness during conductive cooling of the metamorphic pile. Retrograde shear zones record a later northward directed shear (Clarke *et al.*, 1986); they were probably responsible for exposure of the Olary Block at the earth's surface. Although the retrograde shear zones are probably not related to the 'Olarian' Orogeny, the two events sug-

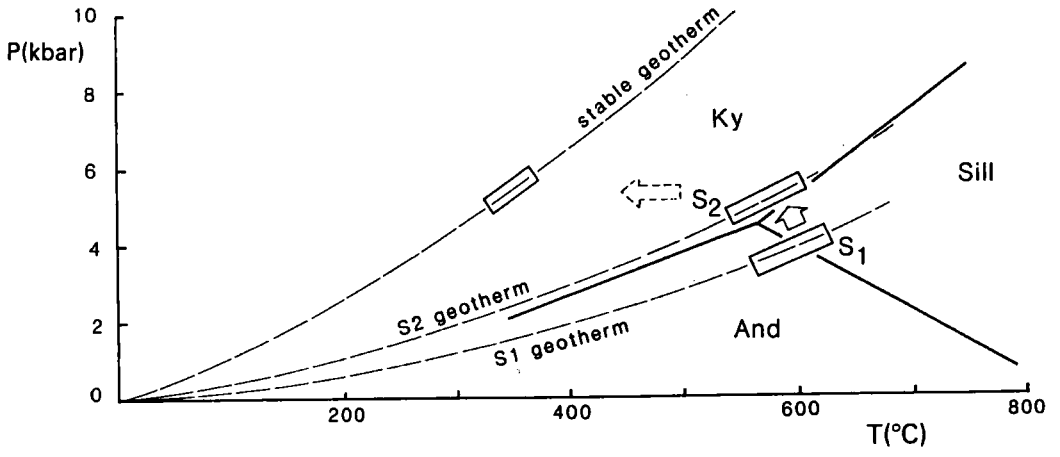

Fig. 5. *P–T* diagram to show possible geotherms at the time of the development of the S_1 and S_2 assemblages. The arrows indicate the anticlockwise *P–T* path.

gest that only compressive tectonic events have been recorded on a regional scale.

Both the Olary Block and the Broken Hill Block appear to show anticlockwise *P–T* paths. The path constructed for the Broken Hill Block (Phillips & Wall, 1981) is based on the presence of high-grade assemblages in metapelites in the southern part of the Block involving sillimanite + cordierite + garnet, which are cut by staurolite + kyanite-bearing retrograde shear zones. Metamorphic grade increases within both the Olary Block and Broken Hill Block in a south to south-eastward direction (Binns, 1964; Spry, 1977; Phillips & Wall, 1981; Hobbs, Archibald, Etheridge & Wall, 1984). The similarity in metamorphic and tectonic history between the two blocks is consistent with their comprising a single orogenic domain, the Willyama Complex. The Willyama Complex is a regional metamorphic terrain and not a localized hotspot in the vicinity of Broken Hill as suggested by Katz (1976). The presently exposed variation in metamorphic grade is best explained by regional block tilting as documented elsewhere, for example, in the Himalayas (Le Fort, 1975), and the Alps (Zingg, 1980), and not by a variation in heat flow.

The location of the S_1 geotherm at lower pressure than the aluminosilicate triple point, namely 4.5 ± 0.5 kbar, 560 ± 25°C (Holland & Powell, 1985) suggests a much more perturbed geotherm than could occur in thickened crust in an England & Richardson (1977) model. Moreover, such models lead to essentially isothermal decompression due to the isostatic response to crustal thickening, rather than the observed further compression. Thus, a radically different tectonic setting is required. Thinning of the mantle lithosphere, thereby steepening the geotherm, is the best way to produce the required thermal metamorphism on a regional scale (Sandiford & Powell, 1986). The flux of heat by convective transfer (Wells, 1980) may aid this process. Extrapolation of the S_1 geotherm defined in Fig. 5 would lead to temperatures in excess of 1000°C at the bottom of a crust of normal thickness, say 35 km. This type of *P–T* environment, followed by grossly isobaric cooling, has been reported for many areas, and seems to be a feature of Precambrian granulite terrains (Sandiford & Powell, 1986). That compression with no, or minor, crustal thickening was recorded by the 'Olarian' Orogeny suggests that metamorphism in this setting was not necessarily related to tectonic processes which were happening concurrently.

The recognized syntectonic granitoids in the Olary Block are not voluminous enough at the exposed tectonic level to contribute to the perturbation of the geotherm, except in the form of local contact effects. Logically, the granitoids were derived at a deeper level in the metamorphic pile, so the suggested geotherms imply considerable temperatures in the lower crust, sufficient to derive granitoids by partial melting. The absence of similar granitoids in the higher grade southern part of the Broken Hill Block makes it tempting to suggest that such rocks may have contributed to melts that were intruded into higher levels of the crust as granitoids. In this southern portion of the Broken Hill Block, however, migmatites are common and detailed studies suggest that more melt is present than could have been internally derived from the enclosing sediments (J. Downes, personal communication, 1986). Thus, in that area, which was only 100–150°C hotter than the highest grade rocks in the Olary Block, there is evidence for addition of melt, pervasively in the migmatites rather than as granitoids in the Olary Block.

ACKNOWLEDGEMENTS

This work was completed whilst Clarke was the recipient of an Australian Commonwealth Postgraduate Research Award, Guiraud a Melbourne University Postgraduate Research Award, and Burg a Melbourne University Research Fellowship. We thank Amdel and the South Australian Department of Mines and Energy for providing some of the rock samples. J. Downes is thanked for discussion during the study, and B. Harte is thanked for discussing the effect of Mn on the KFMASH petrogenetic grid. N. Phillips, B. Hensen and R. Vernon are thanked for critically reviewing earlier versions of the manuscript.

REFERENCES

Bell, T.H. & Rubenach, M.J., 1983. Sequential porphyroblast growth and crenulation cleavage development during progressive deformation. *Tectonophysics*, **92**, 171–194.

Bell, T.H., Rubenach, M.J. & Fleming, P.D., 1986. Porphyroblast nucleation, growth and dissolution in regional metamorphic rocks as a function of deformation partitioning during foliation devel-

opment. *Journal of Metamorphic Geology*, **4**, 37–67.

Binns, R.A., 1964. Zones of progressive regional metamorphism in the Willyama Complex, Broken Hill District, N.S.W. *Journal of the Geological Society of Australia*, **1**, 306–326.

Clarke, G.L., Burg, J.P. & Wilson, C.J.L., 1986. Stratigraphic and structural constraints on the Proterozoic tectonic history of the Olary Block, South Australia, *Precambrian Research*, **34**, 107–138.

England, P.C. & Richardson, S.W., 1977. The influence of erosion upon the mineral facies of rocks from different metamorphic environments. *Journal of the Geological Society of London*, **134**, 201–213.

Etheridge, M.A. & Cooper, J.A., 1981. Rb/Sr isotope and geochemical evolution of a recrystallised shear (mylonite) zone at Broken Hill. *Contributions to Mineralogy and Petrology*, **78**, 74–84.

Etheridge, M.A., Rutland, R.W.R. & Wyborn, L.A.I., 1985. Tectonic processes in the early to middle Proterozoic of Northern Australia. *BMR Record 1985/28* (abs).

Ferguson, A.K. & Sewell, D.K.B., 1980. A peak integration method for acquiring X-ray data for on-line microprobe analysis. *X-ray Spectrometry*, **9**, 48–51.

Forbes, B.G. & Pitt, G.M., 1980. Geology of the Olary Region. *South Australian Department of Mines and Energy*, Report Book. No. BO/151.

Forbes, B.G. & Pitt, G.M., 1987. Geology of the Olary 1:250,000 sheet. *South Australian Department of Mines and Energy* Report, (in press).

Glen, R.A., Laing, W.P., Parker, A.J. & Rutland, R.W.R., 1977. Tectonic relationships between the Proterozoic Gawler and Willyama Orogenic domains, Australia. *Journal of the Geological Society of Australia*, **24**, 124–150.

Harte, B. & Hudson, N.F.C., 1979. Pelite facies series and the temperatures and pressures of Dalradian metamorphism in eastern Scotland. In: *The Caledonides of the British Isles Reviewed* (eds A.L. Harris, C.H. Holland & B.E. Leake), Geological Society of London (Special Publication), **8**, 323–337.

Hobbs, B.E., Archibald, N.J., Etheridge, M.E. & Wall, V.J., 1984. Tectonic history of the Broken Hill Block, Australia. In: *Precambrian Tectonics Illustrated* (eds Kroner, A. & Greiling, R.), pp. 353–368. E. Schweizerbartsche Verlagsbuchhandlung, Stuttgart.

Holland, T.J.B. & Powell, R., 1985. An internally consistent thermodynamic dataset with uncertainties and correlations: 2. Data and results. *Journal of Metamorphic Geology*, **3**, 343–370.

Hudson, N.F.C. & Harte, B., 1985. K_2O poor, aluminous assemblages from the Buchan Dalradian, and the variety of orthoamphibole assemblages in aluminous bulk compositions in the amphibolite facies. *American Journal of Science*, **285**, 224–266.

Katz, M.B., 1976. Broken Hill—A Precambrian hotspot? *Precambrian Research*, **3**, 91–106.

Le Fort, P., 1975. Himalayas: the collided range. Present knowledge of the continental arc. *American Journal of Science*, **275A**, 1–44.

Liverton, T., 1967. The petrology of a uranium bearing adamellite body at Crocker Well, South Australia. *Unpubl. B.Sc.(Hons) thesis, University of Adelaide*.

Ludwig, K.R. & Cooper, J.A., 1984. Geochronology of Precambrian granites and associated U–Ti–Th mineralization, northern Olary province, South Australia. *Contributions to Mineralogy and Petrology*, **86**, 298–308.

Mawson, D., 1912. Geological investigations in the Broken Hill area. *Memoirs of the Royal Society of South Australia*, **11**, 211–319.

Mawson, D. & Sprigg, R.C., 1950. Subdivision of the Adelaide System. *Australian Journal of Science*, **13**, 69–72.

Osberg, P.H., 1971. An equilibrium model for Buchan-type metamorphic rocks, south central Maine. *American Mineralogist*, **56**, 570–586.

Phillips, G.N., 1978. Metamorphism and geochemistry of the Willyama Complex, Broken Hill. *Unpubl. PhD thesis, Monash University*.

Phillips, G.N. & Wall, V.J., 1981. Evaluation of prograde regional metamorphic conditions: their implications for the heat source and water activity during metamorphism in the Willyama Complex, Broken Hill, Australia. *Bulletin de la Société Française de Minéralogie et de Cristallographie*, **104**, 801–810.

Sandiford, M. & Powell, R., 1986. Deep crustal metamorphism during continental extension: modern and ancient examples. *Earth and Planetary Science Letters*, **79**, 151–158.

Sprigg, R.C., 1952. Sedimentation in the Adelaide Geosyncline and the formation of the continental terrace. In: *Sir Douglas Mawson Anniversary Volume* (eds Glaessner, M.F. & Sprigg, R.C.), pp. 153–159. University of Adelaide.

Spry, A.H., 1977. Petrology of the Olary Region, Amdel project 1/1/170, Amdel Report No. 1172. *Unpublished South Australian Department of Mines and Energy*, Open file env. 2466.

Stevens, B.P.J., 1986. Post-depositional history of the Willyama Supergroup in the Broken Hill Block, N.S.W. *Australian Journal of Earth Science*, **3**, 73–98.

Thompson, A.B. & England, P.C., 1984. Pressure–temperature–time paths of regional metamorphism II. Their inference and interpretation using mineral assemblages in metamorphic rocks. *Journal of Petrology*, **25**, 929–955.

Thompson, B.P., 1976. Tectonics and regional geology of the Willyama, Mount Painter and Denison Inliers. In: *Economic Geology of Australia and Papua New Guinea* (ed. Knight, C.L.), pp. 469–475. Australasian Institute of Mining and Metallurgy.

Thompson, J.B., 1957. The graphical analysis of mineral assemblages in pelitic schists. *American Mineralogist*, **42**, 842–858.

Vernon, R.H., 1969. The Willyama Complex, Broken Hill area. *Journal of the Geological Society of Australia*, **16**, 20–65.

Vernon, R.H., 1978. Porphyroblast-matrix microstructural relationships in deformed metamorphic

rocks. *Geologische Rundschau*, **67**, 288–305.
Vernon, R.H. & Ransom, D.M., 1971. Retrograde schists of the amphibolite facies at Broken Hill, New South Wales. *Journal of the Geological Society of Australia*, **18**, 267–277.
Warren, R.G., 1983. Metamorphism and tectonic evolution of granulites, Arunta Block, central Australia. *Nature*, **305**, 300–303.
Wells, P.R.A., 1980. Thermal models for the magmatic accretion and subsequent metamorphism of continental crust. *Earth and Planetary Science Letters*, **46**, 253–265.
Whittle, A.W., 1949. The geology of the Boolcoomata granite. *Transactions of the Royal Society of South Australia*, **72**, 228–243.
Willis, I.L., Brown, R.E., Stroud, W.J. & Stevens, B.P.J., 1983. The Early Proterozoic Willyama Supergroup: stratigraphic sub-division and interpretation of high to low grade metamorphic rocks in the Broken Hill Block, N.S.W. *Journal of the Geological Society of Australia*, **30**, 195–224.
Zingg, A., 1980. Regional metamorphism in the Ivrea Zone (Southern Alps, N-Italy): field and microscopic investigations. *Schweizerische Mineralogische und Petrographische Mitteilungen*, **60**, 153–179.

Received 2 April 1986; revision accepted 11 November 1986